Optical Second Harmonic Generation during the Electrocatalytic Oxidation of Formaldehyde on Pt(111): Potentiostatic Regime versus Galvanostatic Potential Oscillations

Elena Mishina,*,†,‡ Antonis Karantonis,† Qing-Kai Yu,† and Seiichiro Nakabayashi†

Department of Chemistry, Faculty of Science, Saitama University, Saitama 338-8570, Japan, and Moscow Institute of Radioengineering, Electronics and Automation, prosp. Vernadskogo 78, 117454 Moscow, Russia

Received: May 20, 2002; In Final Form: July 11, 2002

The electrocatalytic oxidation of formaldehyde on Pt(111) under potentiostatic conditions and periodic potential oscillations was studied by using optical second harmonic generation (SHG). Under potentiostatic conditions, order−disorder and order−order phase transitions were observed. Under galvanostatic conditions, oscillations of the SHG field occurred, corresponding to the potential oscillations. However, in the dynamic regime only the evidence of a structural order−disorder phase transition is present in SHG data. This might be due to a much higher time constant of the surface ordering in comparison to the oscillation period.

1. Introduction

The history of the studies of electrocatalytic oxidation of small organic molecules on platinum ranges back to the 1960s.[1−4] Among these systems, the oxidation of formic acid in acidic media is one of the most extensively investigated. Combination of polarization-modulated infrared reflection−absorption spectroscopy and electrochemical techniques showed that, in the case of polycrystalline Pt, the main adsorbed species is linearly bonded CO which acts as a catalytic poison.[5,6] Linearly bonded and bridge-bonded CO play the same role in the case of single-crystal Pt electrodes, as was shown by combining single-crystalline electrochemical methods with electrochemically modulated infrared spectroscopy.[7,8] An interesting feature of the electrocatalytic oxidation of formic acid on polycrystalline Pt is that it is accompanied by spontaneous oscillations of the potential (under galvanostatic conditions).[9−12] Spontaneous oscillations of the current also accompany the oxidation of this species on single-crystal Pt under potentiostatic conditions[13−16] (Class IV.2 electrochemical oscillator).[17]

The electrocatalytic oxidation of formaldehyde on Pt electrodes in acidic solutions was found to have many similarities with the above-mentioned system. Infrared and electrochemical mass spectrometry studies showed that linearly bonded and bridge-bonded CO act also as a catalytic poison in the case of polycrystalline[18,19] and single-crystal Pt.[20] Furthermore, this system also exhibits spontaneous potential oscillations[1,21−28] as well as current oscillations (under the presence of a sufficiently large ohmic potential drop).[23]

Despite the large amount of work concerning these two related systems and the valuable information obtained from the combination of electrochemical techniques and IR spectroscopy, the surface structure is still unknown during both static and oscillatory conditions, because the STM technique is not applicable for studies of spatio-temporal dynamics on a sub-second scale. The optical second-harmonic generation (SHG), which is surface and symmetry sensitive, is very useful for studying the structure of surface layers as well as the dynamics of the interface processes.[29−31] The sensitivity of SHG for CO adsorption during the catalytic oxidation of formaldehyde in the potentiostatic regime was shown in the past.[32,33] However, no structural information was obtained in those studies due to the use of a polycrystalline Pt electrode. In the present work, we discuss a series of SHG experiments designed to elucidate the role of adsorbed species and surface structure in the electrocatalytic oxidation of formaldehyde on a Pt(111) electrode in acidic solution.

Because it is now well accepted that CO adsorption plays a crucial role in the process of electrocatalytic oxidation of formaldehyde,[18−20,22,32] the electrochemical CO oxidation on Pt(111) can be considered as a simple submechanism of the present system.[16,34] An SHG study of this process was performed by Akemann et al.[30] In that work, evidence of structural ordering and structural phase transition in a CO layer adsorbed on Pt(111) was given. Hence, the results of Akemann et al. will be considered as a basis for the structural study of the present system. Additionally, we further expand the study by investigating the electrocatalytic oxidation of formaldehyde on Pt(111) under both potentiostatic conditions and spontaneous periodic potential oscillations in the galvanostatic regime.

2. Background

2.1. Electrochemical Oxidation. During the electrochemical oxidation of formaldehyde at a Pt electrode in acidic solutions, two competitive processes take place.[2,21,33] The first is the direct oxidation of HCHO (which exists in aqueous solutions mainly as methylene glycol), where CO_2 molecules are formed and leave the surface. The second is the indirect oxidation occurring through adsorbed CO,

$$CH_2(OH)_2 + * \rightarrow CO_{ad} + H_2O + 2H^+ + 2e^- \qquad (1)$$

where, in the above simplified scheme, the asterisk designates a free Pt site. The final product of the oxidation takes place through the reaction of adsorbed CO and neighboring adsorbed OH (or H_2O).

A typical cyclic voltammogram of the Pt(111)|0.4 M HCHO, 2 M H_2SO_4 system is presented in Figure 1. During the anodic

* Corresponding author. E-mail: elena@chem.saitama-u.ac.jp.
† Saitama University.
‡ Moscow Radioengineering Institute.

10.1021/jp026146x CCC: $22.00
Published on Web 08/31/2002

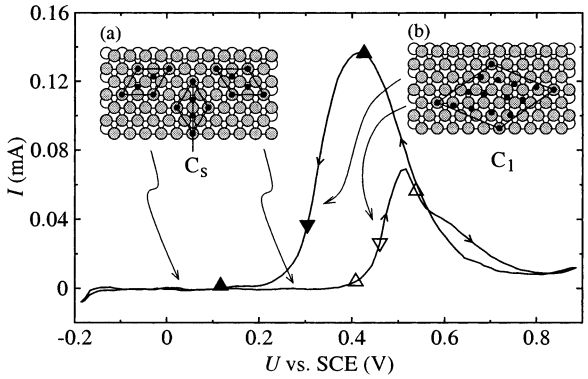

Figure 1. Cyclic voltammogram during oxidation of 0.4 M formaldehyde at Pt(111) in 2 M H_2SO_4. Scan rate 10 mV s^{-1}. Surface structure of CO adsorbed on Pt(111): (a) (2 × 2) with symmetry C_s and (b) ($\sqrt{19} \times \sqrt{19}$) with symmetry C_1. Triangles correspond to characteristic points of the SHG isotropic component, Figure 3a.

scan and at low potentials, CO molecules are dissociatively produced from formaldehyde and adsorb on the Pt surface, eq 1, thus, "poisoning" the electrode and not allowing the direct oxidation of formaldehyde. At higher potentials, OH is probably adsorbed in the neighborhood of CO and reacts with the oxide and both leave the surface through a CO_2 molecule. Thus, the indirect path results in a formation of free sites, giving a way for the direct path. Decreasing the electrode potential makes the direct path preferable until the complete poisoning of the electrode. Competition between the direct and indirect processes leads to the coexistence of adsorbed CO and OH species on the Pt(111) surface on both anodic and cathodic scans, but in different surface concentrations. For rather high concentrations of oxidizable species, the solution serves as a big source of formaldehyde; therefore many more molecules are involved in direct oxidation, providing a higher current (preferable process during the cathodic scan) than for indirect oxidation (preferable process during the anodic scan).

Under galvanostatic conditions these processes give rise to spontaneous potential oscillations whose waveform varies from almost harmonic to chaotic, depending on the current flowing through the system and the surface state.[21,25,28]

2.2. Structural Information. To our knowledge, there is no information about the structure of adsorbed layers during the process of catalytic oxidation of formaldehyde or formic acid. Infrared spectroscopy studies on formaldehyde[20] revealed two types of adsorbed CO, top and bridge, whereas three bands were observed for formic acid, which were assigned to CO adsorbed molecules, on-top, bridge, and hollow.[35] For a CO-saturated solution in perchloric acid, two configurations were proposed, on the basis of STM, IRAS, and SHG measurements:[30,36] for low potentials a (2 × 2) surface (Figure 1a) and for high potentials a ($\sqrt{19} \times \sqrt{19}$) surface structure (Figure 1b). The (2 × 2) structure contains one on-top site and two 3-fold hollow sites whereas the ($\sqrt{19} \times \sqrt{19}$) structure contains one on-top site, six near top sites, and six 2-fold bridge sites. These adsorbed species induce the following static dipole momentum; for on-top sites, $\mu_0^{top} = +0.38$ D, for hollow sites $\mu_0^{hollow} = -0.53$ D, and for bridge sites $\mu_0^{bridge} = -0.34$ D. Therefore the average dipole momentum (for one site) for the (2 × 2) structure is $\mu_0^{2\times2} = -0.23$ D, and the average dipole momentum for ($\sqrt{19} \times \sqrt{19}$) is $\mu_0{}^{\sqrt{19}\times\sqrt{19}} = +0.05$ D. In a vacuum a ($\sqrt{3} \times \sqrt{3}$) surface structure was proposed.[37] However, the model of Villegas and Weaver[36] seems to be more relevant to our study; therefore it will be used for further discussion. Three equal configurations for both reconstructions are possible in regard to three equal ($1\bar{1}0$) crystallographic axes at the surface that are shown for the (2 × 2) structure in Figure 1a (the same holds for the ($\sqrt{19} \times \sqrt{19}$) structure). Generally, they form domains on the surface that could be either compensated or not.

2.3. Optical Details. According to the present status of the theory and interpretation of SHG response from a metal surface in aqueous environment,[31,38] adsorption of species on the surface leads to the change of metal surface susceptibility due to electron density spatial redistribution. Hence, only in the presence of charge transfer (or ionic bond) may the SHG response change noticeably, whereas covalent bonds or physisorption of water make this change undetectable.[39,40] In the present system and at various electrode potentials, different species exist at the surface according to the description of section 2.1. Among them, only CO adsorption is important from the nonlinear-optical point of view because it gives rise to the dipole momentum across the interface and therefore changes the nonlinear-optical susceptibility of the interface.

Although the electrode is covered by adsorbed CO, the system should be considered as a surface "sandwich" structure of, at least, two topmost layers of Pt substrate (which determines the surface symmetry as C_{3v} for bare surface) and an adlayer of CO. For both types of possible surface reconstructions the symmetry of the three-sandwich-layer structure is lower, as shown in Figure 1a,b. The surface structure gives a dipole type surface nonlinear polarization,

$$P_i^{D}(2\omega) = \chi_{ijk} E_j(\omega)\, E_k(\omega) \qquad (2)$$

where $\mathbf{E}(\omega)$ is the electric field of the incident wave and $\hat{\chi}$ is the nonlinear susceptibility tensor.

The surface layer lies on top of a centrosymmetric bulk with quadrupole-type polarization,

$$P_i^{Q}(2\omega) = \gamma \nabla_i(\mathbf{E}(\omega)\cdot\mathbf{E}(\omega)) + \zeta E_i(\omega)\nabla_i E_i(\omega) \qquad (3)$$

where the constants γ and ζ are scale factors for isotropic and anisotropic polarization, respectively. The constant γ can be calculated in the frame of a jellium model as a function of the surface coverage, θ, and the second-order polarizability, μ_2, of an adsorbate/metal system,[39]

$$\gamma(\theta) \propto a_0 + 4\theta e \mu_2 \qquad (4)$$

where e is the absolute electron charge and $a_0 < 0$. The second-order polarizability, μ_2, of an adsorbate−metal system was calculated for some simple molecules and adatoms.[40,41] According to an analytical expression given by Persson and Dubois,[41]

$$\mu_2 = A(\omega)\mu_0{}^3 \qquad (5)$$

where the factor $A(\omega)$ contains, in particular, resonant terms and density of states. In many cases (although not always) far from resonances $A(\omega)$ is a real positive number and thus the sign of zero-order and second-order polarizabilities are coincident.

The nature of the anisotropic bulk constant, ζ, was discussed in the past.[42] It is not sensitive to the normal surface barrier and therefore is not directly dependent on the surface charge (a fact that was recently proved experimentally in a most direct way.[43]) For he (111) surface the SHG field dependence on the

azimuthal angle, Ψ, can be written, under C_{3v} symmetry, as a truncated Fourier expansion,

$$E^{2\omega}(\Psi) = f_0 + c_3 \cos(3\Psi) \quad (6)$$

where f_0 is the total isotropic component and c_3 is the total anisotropic component of the SHG field. It is important to note that, for C_{3v} symmetry, the term f_0 mainly depends on $\gamma(\theta)$ and the normal component of the nonlinear susceptibility, χ_{zzz}, whereas the term c_3 depends only on the in-plane component χ_{xxx} and the potential independent anisotropic factor ζ. CO molecules adsorbed on Pt(111) at different sites possess different zero-order and, therefore, different second-order polarizability. When eqs 4 and 5 are combined, the coverage-dependent term Δf_0 of the isotropic component depends on the respective occupied site coverage, θ^{site}, site = top, bridge, hollow,

$$\Delta f_0 \propto \theta^{\text{top}}(\mu_0^{\text{top}})^3 + \theta^{\text{bridge}}(\mu_0^{\text{bridge}})^3 + \theta^{\text{hollow}}(\mu_0^{\text{hollow}})^3 \quad (7)$$

The term c_3 is sensitive for modification of the surface structure in tangential directions through χ_{xxx}. Therefore its change during adsorption should be proportional to the coverage of the ordered phase and equals zero for a disordered phase, giving in this way the evidence of order−disorder phase transition.

Although first-principle calculations are required for the qualitative analysis of the change of nonlinear susceptibility during adsorption, it was shown[42] that the change of band structure is most important for the anisotropic component. This is why, even for transition metals, a jellium model is generally used[30] for the analysis of the isotropic component and is applied here for the qualitative description of the behavior of γ during phase transitions. At the same time, any kind of phase transition should change the anisotropic component according to the change of the surface band structure.

3. Experimental Section

A Pt(111) single-crystal electrode with diameter 2 mm was prepared by the standard Clavilier method.[44] The quality of the surface was checked by measuring the cyclic voltammogram in a 0.5 M H_2SO_4 aqueous electrolyte. After the checking procedure, a freshly annealed electrode was immersed into an aqueous solution containing 0.4 M of formaldehyde and 2 M of sulfuric acid. Two types of electrochemical regimes were investigated; potentiostatic and galvanostatic. In the first case, standard cyclic voltammograms were measured, whereas in the second case, measurements were performed during potential oscillations.

For the SHG experiments a fundamental radiation of a Ti:Sapphire laser was used, at wavelength 800 nm with a pulse width of about 100 fs and repetition rate of 78 MHz, focused onto a spot of 0.1 mm in diameter at 30° of incidence. SHG radiation at 400 nm was discriminated spectroscopically by appropriate color and band-pass filters. A photon counting system was used for detection. Two types of optical measurements were performed. First, azimuthal dependences were measured in which, for fixed potential, the electrode was rotated around its normal (potentiostatic in sense of electrochemistry). The azimuth angle was measured with respect to one of the $(1\bar{1}0)$ crystallographic axes. Second, for characteristic values of the azimuthal angle (at maximum, $\Psi = 0°$, minimum, $\Psi = 60°$, and intermediate point, $\Psi = 30°$) the SHG intensity was measured during electrode potential scanning or during potential oscillations (potentiostatic and galvanostatic regimes, respectively).

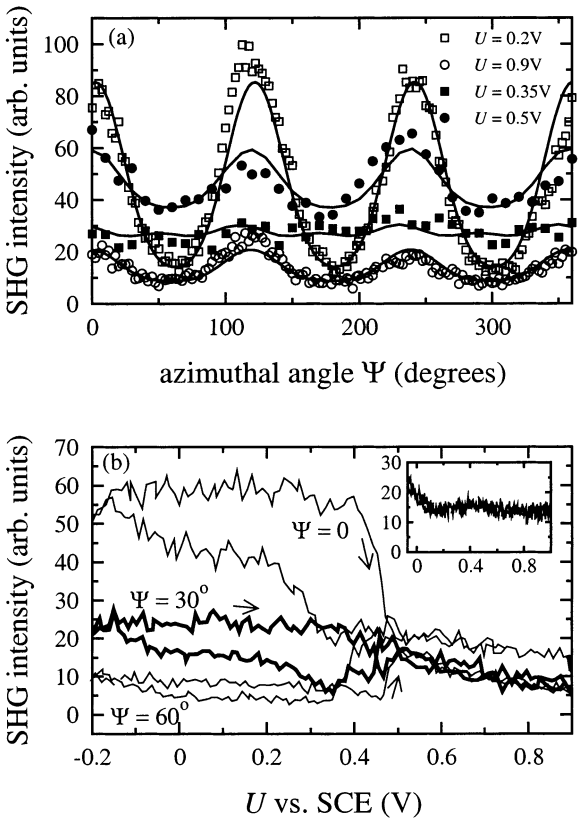

Figure 2. (a) Azimuthal dependence of the SHG intensity at different values of electrode potential. (Lines are fits to data using eq 6.) (b) SHG intensity measured in maximum, minimum, and intermediate points of azimuthal dependence simultaneously with the cycle voltammogram. Inset: SHG intensity at the maximum of rotational anisotropy, $\Psi = 0$, in the absence of HCHO.

4. Results and Discussion

Typical examples of the azimuthal dependence of the SHG intensity for different values of electrode potential are shown in Figure 2a. Figure 2b shows the potential dependences of SHG intensity for characteristic values of the azimuthal angle, Ψ. For reasons of comparison, the inset of Figure 2b shows the SHG intensity at the maximum of rotational anisotropy, $\Psi = 0$, in the absence of HCHO. It can be observed that this curve is almost featureless, indicating that the SHG signal is mainly influenced by adsorbed CO species and not by adsorbed H_2O or OH. This is in accordance with similar observations during the oxidation of CO on Pt(111).[30]

The potential dependences of calculated isotropic and anisotropic components are shown in Figure 3. The isotropic component, f_0, changes almost monotonically during the anodic scan with a local minimum at about 0.45 V (white down-triangle), as can be seen in Figure 3a. In the cathodic scan the changes of the isotropic component are more pronounced with a local maximum at 0.43 V (black up-triangle) and local minimum at 0.3 V (black down-triangle). The anisotropic component, c_3, shown in Figure 3b, and the phase, Δ, between isotropic and anisotropic components, Figure 3c, show steps in both scanning directions.

The decrease of the isotropic component between 0.43 and 0.3 V during the cathodic scan cannot be due to a decrease of CO surface concentration because in this potential region the opposite process takes place; the surface oxide is removed from the surface and Pt free sites are produced on the surface that are finally occupied by CO (in the region between black up-triangles in Figure 1). Below 0.30 V an increase of isotropic

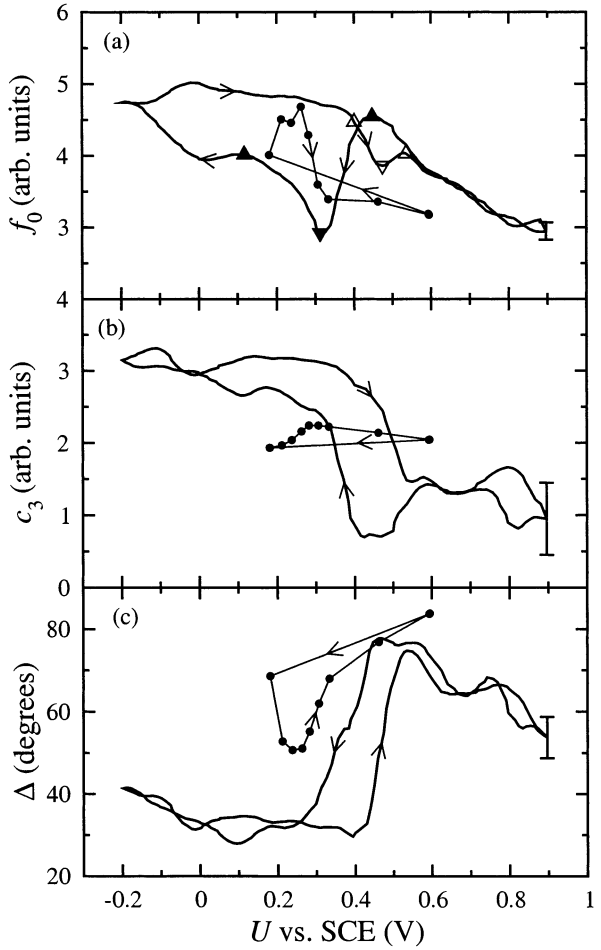

Figure 3. Potential dependence of Fourier components of the SHG field: (a) isotropic component, f_0, (b) anisotropic component, c_3, and (c) phase, Δ. Circles indicate the dependence during potential oscillations (based on temporal dependences of Figure 5). Black and white triangles correspond to characteristic points of f_0 during the cathodic and anodic scan, respectively.

component is observed in agreement with the chemical scenario, i.e., adsorption of CO. The observed contradiction between optical and electrochemical data disappears if a surface phase transition is considered. Actually, for the $(\sqrt{19} \times \sqrt{19})$ surface structure, $\mu_2 \propto \mu_0^3$ and according to eq 4, $|\gamma|$ decreases (because $a_0 < 0$), whereas for the (2×2) surface reconstruction, $\mu_2 < 0$ and $|\gamma|$ increases in comparison with the nonreconstructed metal surface. Thus, a change in a slope between 0.43 and 0.3 V in the potential dependence of the isotropic component, f_0, during the cathodic scan is strong evidence in favor of a change of the sign of second-order polarizability, μ_2. Thus, the following structural scenario emerges from the analysis of the potential dependence of f_0 during the cathodic scan: At 0.43 V, CO adsorption starts as a nucleation and growth process until the highest concentration of $(\sqrt{19} \times \sqrt{19})$ is reached at 0.3 V. This means that an order−disorder phase transition takes place between 0.43 and 0.3 V. Further decrease of the potential causes the formation of the (2×2) phase that is completely formed at ≈0.12 V. Here we must note that in completely static conditions, phase transition takes place at a specific point; however, if the external parameters (in our case the potential) change dynamically, the phase transition appears within a parameter range and hysteresis appears.[45] In particular, these features of SHG behavior during phase transitions were discussed in the past.[46]

In the anodic direction the presence of a positive slope in the potential dependence of the isotropic component around 0.45 V is less pronounced. This might be due to the different conditions for the adsorption/desorption processes of CO; during the anodic scan, the indirect oxidation of formaldehyde is more probable. Therefore, the surface configuration is determined not only by the desorption of CO but also by the adsorption of OH followed by the removal of a neighboring CO molecule. This should completely destroy any ordering of the surface, giving rise to the coadsorption driven order−disorder phase transition. The residual of negative slope in Figure 3a during the anodic scan might be then proportional to the probability of direct oxidation, which increases with the increase of potential (until OH adsorption becomes preferable). This can be seen by comparing the optical response, Figure 3, with the corresponding regions on the electrochemical measurements, Figure 1.

According to symmetry analysis (section 2.3) only formation of ordered structure, including the case of compensated domains, gives rise to a change of anisotropic component. If the overlayer structure is disordered on the molecular level, the anisotropic component does not change. Figure 3b shows a strong change of the anisotropic component that also points to the formation of an ordered phase below 0.43 V. Thus, both isotropic and anisotropic components give evidence of an order−disorder phase transition. There is no change in the anisotropic component during order−order (possibly $(2 \times 2) \rightarrow (\sqrt{19} \times \sqrt{19})$) phase transition, which follows from the data of the isotropic component. This means that the change of the surface band structure is quite small for these two configurations. For further analysis, combined first-principle and microscopic calculations are required similarly to Yamamoto et al.[47]

Finally, it follows from SHG measurements in the potentiostatic regime that, both during the anodic and cathodic scan the symmetry of the surface structure changes due to phase transitions. However, the observed phenomena depend on the scanning direction; during the cathodic scan two types of symmetry changes are clearly observed and are referred, on the basis of STM and SHG measurements for CO oxidation process, to order−disorder phase transition and order−order phase transition. In the anodic scan only the order−disorder phase transition is well pronounced.

Figure 4 shows the results of electrochemical and SHG studies on the system under galvanostatic conditions for $I = 72$ μA. The SHG signal is measured at maximum, minimum, and intermediate points ($\Psi = \pi/6$) of azimuthal dependence. From the time series one can see that the SHG intensities at maximum (Figure 4a) and intermediate points (Figure 4b) are out of phase with the potential oscillations whereas at the minimum point the intensity is almost in phase (Figure 4c). These data allow the calculation of the isotropic and anisotropic components, based on eq 6. The calculation results within one period with $T \approx 1.5$ s are shown in Figure 5. Note that all data presented in this figure are averaged over 10 oscillation periods to increase the signal-to-noise ratio of the SHG measurements and that $T \approx 1.5$ s was the maximum period of oscillations with sufficient amplitude obtained in our system.

Qualitatively, galvanostatic data fall in agreement with potentiostatic data in the range of instability; f_0 is maximal for minimum potential (maximal CO coverage), Figure 5b, and the opposite relation holds for the phase, Δ, Figure 5d. However, when plotted simultaneously, potentiostatic and galvanostatic data reveal an obvious difference, as can be seen in Figure 3. The amplitudes of the changes of the SHG Fourier components under galvanostatic conditions are much smaller than in

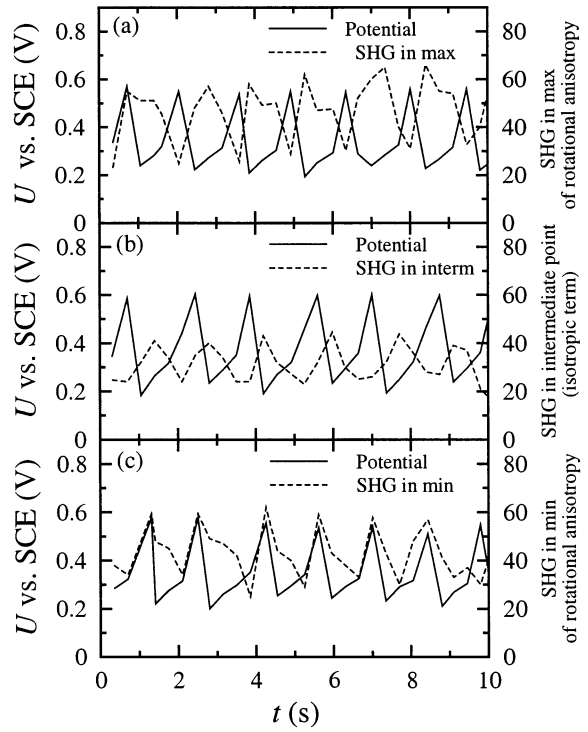

Figure 4. Simultaneous electrochemical and SHG measurements under galvanostatic oscillations in (a) maximum, (b) intermediate, and (c) minimum points of azimuthal dependence. $I = 72\ \mu$A.

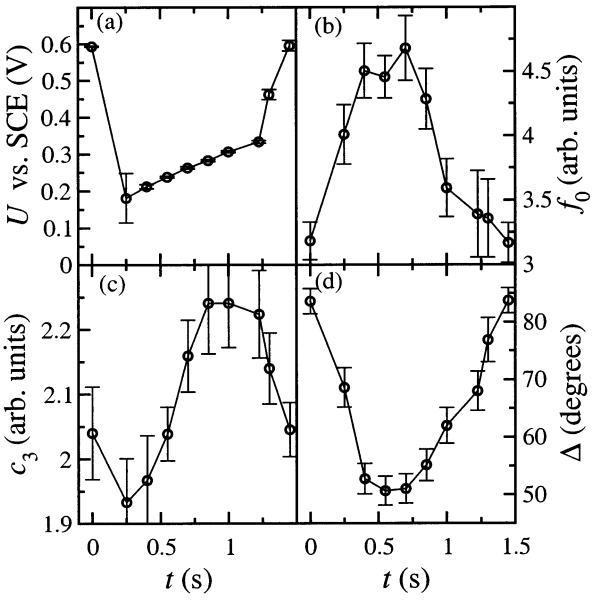

Figure 5. Temporal dependence of (a) the potential, *U*, (b) the isotropic component, f_0, (c) the anisotropic component, c_3, and (d) the phase, Δ, within one period. $I = 72\ \mu$A.

potentiostatic conditions (50% for isotropic and 10% for anisotropic components, respectively, from their potentiostatic values).

The theoretical model of Okamoto et al.[48] for the oscillatory oxidation of formic acid (a system similar to the present one) predicted that CO coverage oscillates in the range ≈0.15 to ≈0.2, never reaching 0 or 1 as in the potentiostatic regime. (A similar result, but under potentiostatic oscillations was obtained by Strasser et al.[34]) Based on this model and on SHG data, the following structural model could be introduced. Not all CO molecules are involved in the dynamic process, which occurs on a background of stable (ordered) surface structure. This is why the change of the anisotropic component is very small (Figure 3b) revealing a decrease of ordering in the end of the period (Figure 5c). Time-resolved IRAS measurements[30] showed that complete formation of the ordered structure takes 50−100 s, that is more than an order of magnitude longer than the period of the oscillations in the present study. It is very probable that during one period, the surface is not able to relax to a stable ordered structure. Nevertheless, the increase of c_3 (increase of ordering) appears in the slower part of oscillation, as can be seen in Figure 5c. One should notice that under galvanostatic conditions the transition from high to low potentials (corresponding to the cathodic scan of the potentiostatic experiments) is very fast. At the present, the sensitivity of the SHG setup does not offer adequate temporal resolution within this transition. During the transition from low to high potentials (corresponding to the anodic scan of the potentiostatic experiments) the behavior of the isotropic component confirms the presence of an order−disorder phase transition similar to the one observed under potentiostatic conditions but with lower CO concentration involved in the process.

Finally, it must be noted that from SHG data, only the change of symmetry can be observed. For the exact assignment of the observed anisotropy to the surface configuration, STM data are required.

5. Conclusions

We studied the process of catalytic oxidation of formaldehyde on Pt(111) under potentiostatic and galvanostatic conditions, using SHG. Under potentiostatic conditions, two surface phase transitions were observed: order−disorder and order−order. These phase transitions are similar to those observed previously at Pt(111) for CO-saturated electrolyte.[30] Under galvanostatic conditions, oscillations of the SHG field were observed corresponding to the potential oscillations. During the spontaneous transition from low to high potentials an order−disorder phase transition was observed, similar to the one observed under potentiostatic conditions but with lower CO concentration involved in the process. However, in the dynamic regime the evidence of a structural order−order phase transitions is absent in SHG data. This might be due to a much higher time constant of the surface ordering in comparison to the oscillation period. The SHG measurements presented in this work give the first evidence of structural ordering during formaldehyde oxidation not only under potentiostatic conditions but also during galvanostatic oscillations.

Acknowledgment. This work was supported by the Research for the Future (RFTF) Program of the Japanese Society for the Promotion of Science. The authors thank Dr. A. V. Petukhov for useful discussions.

References and Notes

(1) Buck, R. P.; Griffith, L. R. *J. Electrochem. Soc*. **1962**, *109*, 1005.
(2) Hunger, H. F. *J. Electrochem. Soc.* **1968**, *115*, 492.
(3) Hunger, H. F. *J. Electrochem. Soc*. **1969**, *116*, 1519.
(4) Wojtowicz, J.; Marincic, N.; Conway, B. E. *J. Chem. Phys*. **1968**, *48*, 4333.
(5) Kunimatsu, K. *J. Electroanal. Chem*. **1986**, 213.
(6) Kunimatsu, K.; Kita, H. *J. Electroanal. Chem.* **1987**, 218.
(7) Clavilier, J.; Sun, S. G. *J. Electroanal. Chem*. **1986**, *199*, 471.
(8) Sun, S. G.; Clavilier, J.; Bewick, A. *J. Electroanal. Chem*. **1988**, *240*, 147.
(9) Okamoto, H. *Electrochim. Acta* **1992**, *37*, 37.
(10) Inzelt, G.; Kertész, V. *Electrochim. Acta* **1993**, *38*, 2385.
(11) Kertész, V.; Inzelt, G.; Barbero, C.; Kötz, R.; Haas, O. *J. Electroanal. Chem*. **1995**, *392*, 91.
(12) Albahadili, F. N.; Schell, M. *J. Electroanal. Chem*. **1991**, *308*, 151.

(13) Markovic, N.; Ross, Ph. N. *J. Phys. Chem.* **1993**, *97*, 9711.
(14) Raspel, F.; Eiswirth, M. *J. Phys. Chem.* **1994**, *98*, 7613.
(15) Schmidt, T. J.; Grgur, B. N.; Markovic, N. M.; Ross, P. N. *J. Electroanal. Chem*. **2001**, *500*, 36.
(16) Strasser, P.; Lübk, M.; Raspel, F.; Eiswirth, M.; Ertl, G. *J. Chem. Phys*. **1997**, *107*, 979.
(17) Strasser, P.; Eiswirth, M.; Koper, M. T. M. *J. Electroanal. Chem*. **1999**, *478*, 50.
(18) Nishimura, K.; Ohnishi, R.; Kunimatsu, K.; Enyo, M. *J. Electroanal. Chem*. **1989**, *258*, 219.
(19) Solomun, T. *Surf. Sci*. **1986**, *176*, 593.
(20) Sun, S. G.; Lu, G. Q.; Tian, Z. W. *J. Electroanal. Chem*. ***1995***, 393, 97.
(21) Xu, Y.; Schell, M. *J. Phys. Chem.* **1990**, *94*, 7137.
(22) Okamoto, H.; Tanaka, N. *Electrochim. Acta* **1993**, *38*, 503.
(23) Koper, M. T. M.; Hachkar, M.; Beden, B. *J. Chem. Soc., Faraday Trans*. **1996**, *92*, 3975.
(24) Okamoto, H.; Tanaka, N.; Naito, M. *J. Phys. Chem. A* **1997**, *101*, 8480.
(25) Okamoto, H.; Tanaka, N.; Naito, M. *J. Phys. Chem. A* **1998**, *102*, 7343.
(26) Okamoto, H.; Tanaka, N.; Naito, M. *J. Phys. Chem. A* **1998**, *102*, 7353.
(27) Okamoto, H.; Tanaka, N.; Naito, M. *J. Electrochem. Soc*. **2000**, *147*, 2629.
(28) Schell, M.; Albahadily, F. N.; Safar, J.; Xu, Y. *J. Phys. Chem.* **1989**, *93*, 4806.
(29) Mishina, E.; Ohta, N.; Yu, Q.-K.; Nakabayashi, S. *Surf. Sci*. **2001**, *494*, L748.
(30) Akemann, W.; Friedrich, K. A.; Stimming, U. *J. Chem. Phys*. **2000**, *113*, 6864.
(31) Lipkowski, J.; Stolberg, L.; Yang, D.-F.; Pettinger, B.; Mirwald, S.; Henglein, F.; Kolb, D. M. *Electrochim. Acta* **1994**, *39*, 1045.
(32) Nakabayashi, S.; Sugiyama, N.; Yagi, I.; Uosaki, K. *Chem. Phys*. **1996**, *205*, 269.
(33) Nakabayashi, S.; Yagi, I.; Sugiyama, N.; Tamura, K.; Uosaki, K. *Surf. Sci*. **1997**, *386*, 82.
(34) Strasser, P.; Eiswirth, M.; Ertl, G. *J. Chem. Phys*. **1997**, *107*, 991.
(35) Iwasita, T.; Nart, F. C.; Lopez, B.; Vielstich, W. *Electrochim. Acta* **1992**, *37*, 2361.
(36) Villegas, I.; Weaver, M. J. *J. Phys. Chem.* **1994**, *101*, 1648.
(37) Ertl, G.; Neumann, M.; Streit, K. M. *Surf. Sci*. **1977**, *64*, 393.
(38) Robinson, J. M.; Richmond, G. L. *Electrochim. Acta* **1989**, *34*, 1639.
(39) Dzhavakhidze, P. G.; Kornyshev, A. A.; Liebsch, A.; Urbakh, M. *Phys. Rev. B* **1992**, *45*, 9339.
(40) Rebentrost, F. *Prog. Surf. Sci*. **1995**, *48*, 71.
(41) Persson, B. N. J.; Dubois, L. H. *Phys. Rev. B* **1989**, *39*, 8220.
(42) Petukhov, A. V. *Surf. Sci*. **1996**, 34z7, 143.
(43) Simpson, L. J.; Furtak, T. E. *J. Electroanal. Chem*. **2001**, *500*, 163.
(44) Clavilier, J.; Faure, R.; Guinet, G.; Durand, R. *J. Electroanal. Chem.* **1980**, *107*, 205.
(45) Ma, Sh.-K. *Modern Theory of Critical Phenomena*; W. A. Benjamin: Reading, MA, 1976.
(46) Kolb, D. B. *Prog. Surf. Sci*. **1996**, *51*, 109.
(47) Yamamoto, M.; Kinoshita, M.; Kakiuchi, T. *Electrochim. Acta* **2000**, *46*, 165.
(48) Okamoto, H.; Tanaka, N.; Naito, M. *Chem. Phys. Lett*. **1996**, *248*, 289.